Control over binding stoichiometry and specificity in the supramolecular immobilization of cytochrome *c* on a molecular printboard

Manon J. W. Ludden,[a] Jatin K. Sinha,[b] Gunther Wittstock,*[b] David N. Reinhoudt[a] and Jurriaan Huskens*[a]

Received 10th December 2007, Accepted 25th February 2008
First published as an Advance Article on the web 14th March 2008
DOI: 10.1039/b718940k

Here, the stepwise assembly of an electroactive bionanostructure on a molecular printboard is described. The system consists of a cyclodextrin receptor monolayer (molecular printboard) on glass, a divalent linker, streptavidin (SAv), and biotinylated cytochrome *c* (cyt *c*). The divalent linker consists of a biotin moiety for binding to SAv and two adamantyl moieties for supramolecular host–guest interaction at the cyclodextrin molecular printboard. The binding of biotinylated cyt *c* onto a SAv layer bound to preadsorbed linker appeared to be highly specific. The coverages of cyt *c* as assessed by UV–vis spectroscopy and scanning electrochemical microscopy (SECM) appeared to be identical indicating that all cyt *c* units remained active. Moreover, the coverage values corresponded well with an estimate based on steric requirements, and the binding stoichiometry was therefore found to be by two biotin moieties of cyt *c* per one SAv molecule.

Introduction

The attachment of electro-active proteins at surfaces has resulted in the characterization of several enzymes, and the development of sensing devices based on these proteins.[1–4] Cytochrome *c* (cyt *c*) is a small (12.2 kDa) redox protein with one heme centre, that has been studied extensively.[5–7] The redox potentials of the different class (I) cyt *c* vary between +200 and +350 mV (*vs.* SHE).[7–9] Heme, which is the iron complex of protoporphyrin IX, is a rigid and planar molecule, having four pyrrole groups which are linked by methylene bridges to form a tetrapyrrole ring. The heme group in cyt *c* is covalently bound to the polypeptide chain. An important function of cyt *c* is the electron transfer between cytochrome *c* reductase and cytochrome *c* oxidase. The adsorption of cyt *c* to SAMs has been studied before.[10–12] Fragoso *et al.* for instance have described the surface immobilization of cyt *c* to β-cyclodextrin (βCD) SAMs on Ag *via* adamantyl moieties incorporated in the protein. They showed that cyt *c*, when bound in a supramolecular fashion to a surface, is more stable than cyt *c* physisorbed to a surface.[13]

βCD is a well known host for various small hydrophobic organic molecules in aqueous environments.[14] βCD has been modified by us in order to obtain ordered and densely packed self-assembled monolayers (SAMs) on gold.[15] It is also possible to prepare monolayers of βCD on glass, in that case using a multistep covalent approach.[16] All guest-binding sites in βCD monolayers are equivalent and independent.[17] The use of multivalent host–guest interactions allows the formation of kinetically stable assemblies, and thus local complex formation *e.g.* by patterning, so that these surfaces can be viewed as "molecular printboards".[15,18,19]

Recently, we have introduced the use of βCD molecular printboards as a general platform for protein immobilization by small multivalent, orthogonal linker molecules.[20,21] Streptavidin (SAv) was immobilized in a stepwise fashion to the molecular printboard, allowing heterofunctionalization of the upper biotin-binding pockets.[20] Furthermore, nonspecific interactions could be suppressed completely through the use of a monovalent competitor.[21] The molecular printboard concept thus provides a powerful tool to control the specificity, orientation, binding strength, and coverage of protein attachment through the design of small linker molecules.

Here we will show the controlled attachment of the functional protein cyt *c*. We will show that the interaction between cyt *c* and supramolecularly surface-immobilized SAv is specific. The preservation of electrochemical function of the immobilized cyt *c* after adsorption will be shown by UV–vis absorption and by scanning electrochemical microscopy (SECM), both of which allows the determination of the surface coverage, and thus allows evaluation of the involved binding stoichiometries and steric requirements.

Results and discussion

The building blocks used in this study are depicted in Fig. 1. The synthesis of the divalent linker (**3**) has been described before, as well as the attachment of SAv to the molecular printboard and the heterofunctionalization of the surface-immobilized SAv.[20,21]

The attachment of biotinylated cyt *c* (bt-cyt *c*) to βCD SAMs is envisaged as depicted in Scheme 1. The biotinylation of cyt *c* was performed according to literature procedures with biotin-LC-NHS, which has a spacer arm of 2.24 nm, and will react to free amino positions at the surface of the protein.[22] The reaction mixture contained a 15-fold excess of biotin linker relative to protein, thus probably leading to cyt *c* modified with multiple biotin moieties.

[a]*Molecular Nanofabrication group, MESA+ Institute for Nanotechnology, University of Twente, P.O. Box 217, 7500 AE Enschede, The Netherlands. E-mail: j.huskens@utwente.nl; Fax: (+31) 53-489-4645*
[b]*Department of Chemistry and Institute of Chemistry and Institute of Chemistry and Biology of the Marine Environment, Carl Von Ossietzky University of Oldenburg, PF 2503, D-2611 Oldenburg, Germany. E-mail: gunther.wittstock@uni-oldenburg.de; Fax: (+49) 441-798-3979*

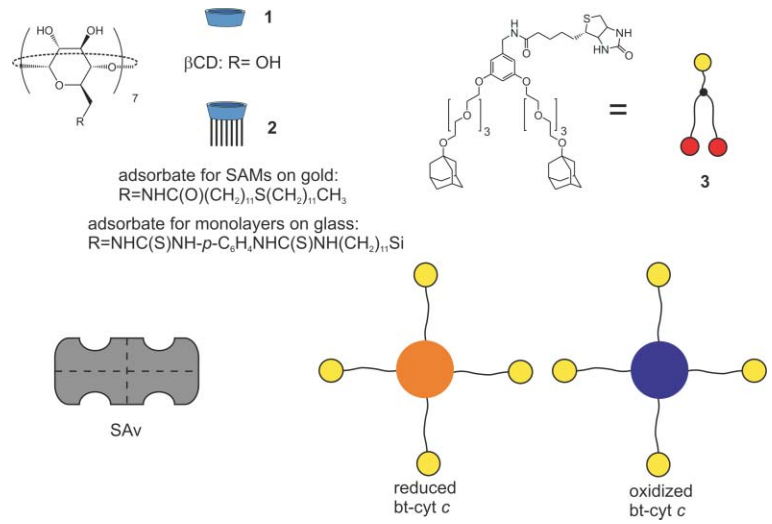

Fig. 1 Building blocks used in this study: βCD (**1**), adsorbate for preparing βCD SAMs (**2**), divalent linker (**3**), SAv (**4**), and bt-cyt *c* (**5**).

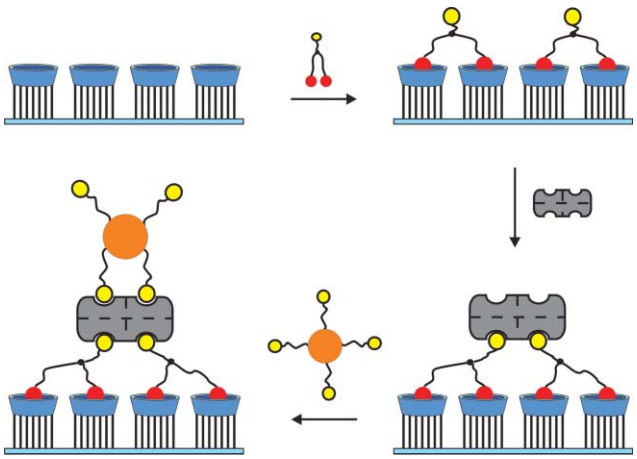

Scheme 1 Stepwise adsorption of **3** and SAv to a βCD SAM, followed by the heterofunctionalization with bt-cyt *c*.

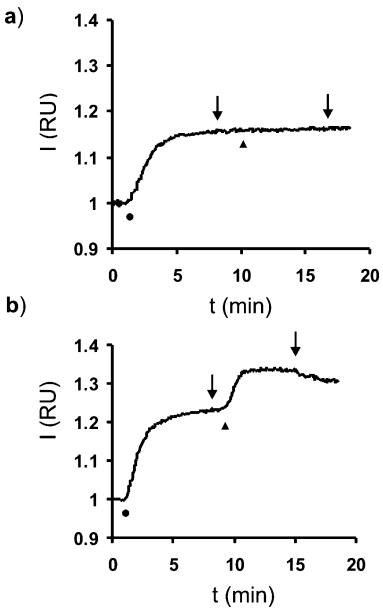

Fig. 2 SPR sensograms of the adsorption of SAv to a **3**-covered βCD SAM, followed by either non-biotinylated cyt *c* (a) or bt-cyt *c* (b). Symbols indicate switching flows to: (●) SAv (in PBS containing 1 mM βCD), (▲) cyt *c* or bt-cyt *c* (in PBS containing 1 mM βCD) for case a and b, respectively, (↓) PBS containing 1 mM βCD.

To test the specificity of bt-cyt *c* binding to the SAv layer, surface plasmon resonance (SPR) experiments were performed, in which SAv was immobilized to a βCD SAM on gold *via* **3** (*ex-situ*), and then, in separate experiments, cyt *c* and bt-cyt *c* were flowed over the surface (Fig. 2). From both sensograms depicted in Fig. 2, SAv adsorption can be clearly observed. The subsequent flow of cyt *c*, however, did not result in an increase in signal intensity, therefore it can be concluded that cyt *c* was not adsorbed onto the SAv layer (Fig. 2a). In the second experiment, an increase in signal intensity was observed upon adsorption of bt-cyt *c* (Fig. 2b). This intensity change was reduced somewhat after rinsing with PBS containing 1 mM βCD, which is attributed to the removal of non-specifically adsorbed bt-cyt *c*. This leads to the conclusion that bt-cyt *c* attaches to the SAv layer employing the strong, specific SAv–biotin interaction.

In order to verify the stoichiometry of the binding scheme shown in Scheme 1, the coverage of bt-cyt *c* was determined by UV–vis and electrochemistry. Cyt *c* displays a Soret band in UV–vis with a peak maximum at $\lambda = 408$ nm which shifts to lower wavelengths upon denaturation.[23] The biotinylated cyt *c* used here has an ε of 2.8 $cm^2\ mg^{-1}$ at 408 nm, as determined by UV–vis spectroscopy in solution (data not shown). In order to determine the surface coverage of bt-cyt *c*, βCD monolayers on glass were covered on both sides with divalent linker by immersion in a 1×10^{-4} M solution of **3**, followed by adsorption of SAv, and finally bt-cyt *c* was attached. UV–vis spectra (Fig. 3) on stacks of four or five samples were recorded. Fig. 3 clearly shows the presence of the Soret band. The signal-to-noise ratio of the data is, however, too low to conclude on the exact position of the peak maximum and thus on the state of the protein. The absorbance (A) at 408 nm was used for the assessment of the cyt *c* coverage using the ε value determined in solution. Thus, a surface coverage of approximately 2×10^{-11} mol cm^{-2} was determined, which is in agreement with the electrochemistry data presented below.

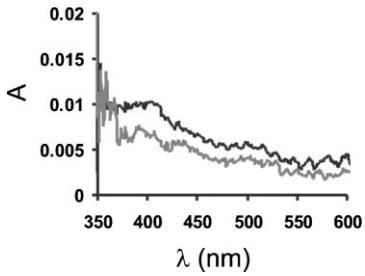

Fig. 3 UV–vis spectra of 8 (–) or 10 (–) βCD SAMs on glass substrates covered with bt-cyt *c* on SAv on **3**, addressed by measuring transmission through 4 or 5 doubly coated glass substrates simultaneously, respectively.

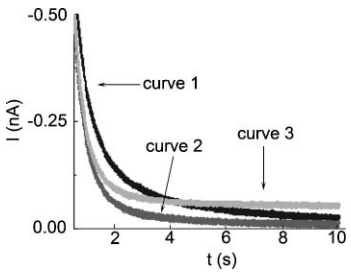

Fig. 4 SECM amperograms in which pulse times are in each case 10 s; (curve 1) first pulse 10 μm from the surface, (curve 2) second pulse 10 μm from the surface, (curve 3) third pulse 300 μm from the surface.

SECM studies on bt-cyt *c* attached to SAv were performed in order to determine the surface coverage of cyt *c* in an electrochemical manner. Therefore, glass substrates with bt-cyt *c* were prepared as described above, now using oxidized cyt *c*. The sample was mounted in an SECM setup, which used a Ag/AgCl reference electrode and a disk-shaped carbon ultramicroelectrode (UME) of 7 μm (Scheme 2). The redox reactions that occur at the UME and at the surface are listed in Scheme 2b. The SECM experiments on βCD SAMs are a modification of the route developed before for ferrocene-terminated dendrimers, which had to be optimized because a monolayer of cyt *c* offers much less redox equivalents.[24]

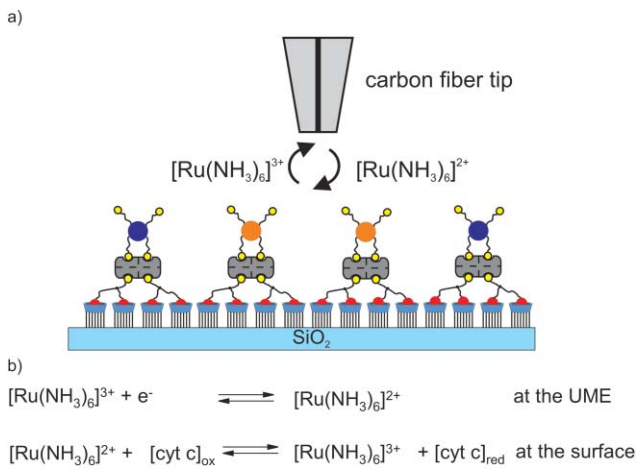

Scheme 2 (a) Schematics of the SECM experiment. $[Ru(NH_3)_6]^{3+}$ is reduced at the tip and diffuses to the molecular printboard where it reduces (oxidized) bt-cyt *c*. Thereafter, $[Ru(NH_3)_6]^{3+}$ diffuses back to the UME, which results in a negative feedback current. (b) Redox reactions taking place at the UME and at the surface.

The UME was positioned at a distance d of 10 μm from the surface and a potential pulse of E_T −0.35 V was applied to the UME in order to reduce the mediator $[Ru(NH_3)_6]^{3+}$. Chronoamperograms of the UME current were recorded during the pulse. This sequence was repeated multiple times at the same location and at different distances from the surface while the horizontal position was not changed (Fig. 4).

First, a 10 s pulse was applied to the UME positioned 10 μm above the surface (Fig. 4, curve 1). The pulse was repeated at the same location (Fig. 4, curve 2). For reference purposes, another pulse experiment was performed far away from the surface (Fig. 4, curve 3).[25,26] Almost all cyt *c* is reduced within the first pulse of about 10 s by a bimolecular electron transfer reaction between $[Ru(NH_3)_6]^{2+}$ and oxidized cyt *c* (Fig. 4, curve 1). During this reaction $[Ru(NH_3)_6]^{3+}$ is regenerated. After diffusion to the UME, it enhances the UME current compared to the same pulse experiment above an inert sample at which no reaction of the mediator is possible. However, the bimolecular reaction can only be sustained as long as *oxidized* cyt *c* is available at the surface. Therefore a second pulse at the same location produces much lower currents (Fig. 4, curve 2). This chronoamperogram is identical to one obtained at the same distance above a bare glass sample. It can be considered a background signal. For times < 0.1 s it results from double layer charging currents and for longer times it is controlled by the hindered diffusion of $[Ru(NH_3)_6]^{3+}$ from the solution bulk through the gap between UME and sample to the active UME area. Curve 1 and curve 2 merge at around 10 s indicating the time when the oxidized cyt *c* is exhausted during the first pulse. The current resulting from hindered diffusion (Fig. 4, curve 2) depends on the distance between the UME and its insulating sheaths to the sample. If the working distance is enlarged (Fig. 4, curve 3), the diffusion is less effectively hindered and the currents are larger than in Fig. 4, curve 2. However, for $t < 4$ s, the currents during the first pulse at 10 μm distance (Fig. 4, curve 1) are *larger* than the currents at large distances (Fig. 4, curve 3). This is a clear proof that the enhancement of the UME currents in curve 1 is a result of the chemical mediator recycling at the substrate surface. The electrical charge Q used to convert the cyt *c* at the surface was obtained by integrating the current difference between the first and the second pulse at $d = 10$ μm distance (curve 1 minus curve 2). The radius r_S of the sample region that is affected by the oxidation can be approximated by considering the average diffusion length of the $[Ru(NH_3)_6]^{2+}$ generated at the UME (Fig. 5). With the known diffusion coefficient of $D = 7.4 \times 10^{-6}$ cm^2 s^{-1},[27] the average diffusion length within the pulse time τ is $(2D\tau)^{\frac{1}{2}}$ and the modified radius at the sample is:

$$r_S = (2D\tau - d^2)^{1/2} \quad (1)$$

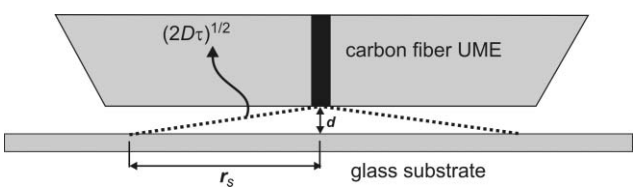

Fig. 5 Estimation of the radius of the modified sample region by the diffusion of the UME-generated $[Ru(NH_3)_6]^{2+}$.

Table 1 Calculation of the surface concentration of cyt *c* from five independent SECM pulse experiments; for all experiments: $r_T = 3.5$ μm, $d = 10$ μm, $D = 7.4 \times 10^{-6}$ cm^2 s^{-1}

τ/s	$Q/10^{-9}$ As[a]	r_S/μm[b]	$\Gamma/10^{-11}$ mol cm^{-2}[c]
5	0.402	85.44	1.82
10	0.707	121.2	1.59
10	1.23	121.2	2.76
10	1.05	121.2	2.36
20	2.04	171.7	2.28

[a] Integrated difference of chronoamperometric currents of the first and the second pulses. [b] Calculated according to eqn (1). [c] Calculated according to eqn (2).

From r_S the modified area can be estimated as $A = \pi r_S^2$. From Q, r_S, the number, n (= 1), of transferred electrons per cyt *c* molecule, and the Faraday constant F, the surface coverage Γ is obtained:

$$\Gamma = Q/(n\,F\,\pi\,r_S^2) \quad (2)$$

The estimation according to eqn (1) and (2) led to a value of $\Gamma = (2.2 \pm 0.5) \times 10^{-11}$ mol cm^{-2} (Table 1). This value compares well with the surface concentration determined by UV–vis (see above). This confirms that all or most of the cyt *c* units are electrochemically functional and accessible when immobilized according to this supramolecular assembly scheme.

From the steric requirements of all building blocks of the bionanostructure, the following picture regarding coverage and stoichiometry can be drawn. The coverage of the βCD SAMs on glass is not exactly known, but is expected to be comparable to the coverage on gold (8×10^{-11} mol cm^{-2}),[28] because the multivalent binding behavior is identical.[16] SAv (2.5 nm × 3 nm × 5 nm) interacts *via* two binding pockets with two divalent linker molecules, each occupying two βCD cavities on the surface (thus reaching a coverage of 4×10^{-11} mol cm^{-2}), and thus a SAv coverage of 2×10^{-11} mol cm^{-2} is expected. Thus the projected area of cyt *c*, a globular protein with dimensions of less than 2 nm,[29] is smaller than the area per biotin-binding site of SAv.[30] However, the biotin-binding pockets on SAv are positioned 2 nm from each other.[31] Thus, one SAv can accommodate one or two cyt *c* molecules, and therefore a coverage of cyt *c* is expected between 2×10^{-11} and 4×10^{-11} mol cm^{-2}. The values found by UV and SECM correspond quite well to this range. Most likely, since the measured values are at the lower limit of this range, the majority of the cyt *c* molecules interacts with two biotin moieties to the SAv layer, in agreement with the biotinylation method leading to the introduction of multiple biotin moieties. The overall stoichiometry picture is sketched in the final structure of Scheme 1.

Comparable systems in which cyt *c* was bound to a SAv layer showed an excess of cyt *c* at the surface after immobilization.[32] The SAv layer formed on top of a biotinylated surface consisted of 2.6×10^{-12} mol cm^{-2} SAv molecules, and 8.8×10^{-12} mol cm^{-2} cyt *c*. On a molecularly flat surface, the theoretical coverage of cyt *c* corresponds to 2.2×10^{-11} mol cm^{-2}.[33] The non-specifically bound cyt *c* was attributed to bad packing of the SAv layer (which was only 60% of a fully packed layer) which allowed cyt *c* to be nonspecifically immobilized at the biotin SAM.[32] In our case, we have excellent control over the packing of the SAv layer, probably owing to the dynamic supramolecular interactions applied in our system, and a notable absence of nonspecific adsorption.

Conclusions

In conclusion, we have shown that the supramolecular binding strategy employed here allows control over binding stoichiometry and specificity, with complete retention of (electrochemical) function. The heterofunctionalization of SAv, allowed by the stepwise buildup *via* the multivalent linker, led to the highly specific binding of bt-cyt *c*. The coverage of cyt *c* is in full agreement with the expected binding stoichiometry of the resulting bionanostructure, which shows that it can be in principle controlled through the design and use of linker molecules with other valencies.[20] The printboard concept described here may eventually be applied in the development of biosensors and chip-based assays, as the stepwise buildup offers control and flexibility over stoichiometry and specificity, and thus over coverage and function.

Experimental

General

All materials and reagents were used as received, unless stated otherwise. The synthesis of **3** has been reported previously.[20] Per-6-amino-β-cyclodextrin was synthesized as described before.[34] Cytochrome *c* was bought at Sigma and biotinylated with Sulfo-NHSLC-biotin (Pierce) according to literature procedures.[22]

Monolayer preparation

Gold substrates for SPR (BK7 glass/2–4 nm Ti/50 nm Au) were obtained from SSens B.V., Hengelo, the Netherlands. βCD monolayers on gold (SPR) and glass (UV–vis and SECM) were prepared as described by our group earlier.[16,35]

SPR

SPR measurements were performed on a Resonant Probes GmbH SPR instrument as described before.[21] Before SPR experiments, **3** was adsorbed at βCD SAMs on gold from a 1×10^{-4} M solution. In the SPR experiments phosphate buffered saline (PBS) was used at pH 7.5. Protein concentrations used throughout the experiments were 1×10^{-7} M. When switching to different solutions throughout the experiment, the flow pump was stopped, and started again after the solution change.

UV–vis spectroscopy

βCD monolayers on glass substrates were subsequent immersed in a 1 mM solution of **3**, a 1×10^{-7} M SAv solution, and finally in a 10^{-7} M solution of bt-cyt *c*. In between these steps a rinse step with PBS buffer was applied. The substrates were carefully rinsed with PBS buffer, and dried in a stream of N_2. Four or five glass substrates, that means 8 or 10 cyt *c*-modified SAMs, were placed in a Varian Cary 300 Bio instrument which was set in the double beam mode, using 5 non-covered glass substrates as a reference. The substrates were placed perpendicular to the beam, and the glass substrates covered the whole area of the beam.

SECM

A home-built SECM was used consisting of a stepper motor positioning system (Märzhäuser, Wetzlar, Germany) and a CHI701

potentiostat (CH Instruments, Austin, TX, USA). Experiments were carried out in a three-electrode configuration and were operated *via* home-built software. The carbon fiber UME (working electrode) had a radius $r_T = 3.5$ μm and the $RG = r_{glass}/r_T = 30$ (r_{glass} is the radius of the insulating glass shielding). A Pt wire served as auxiliary electrode, and was used together with a Ag/AgCl reference electrode, to which all potentials are referred to. Measurements were performed with βCD monolayers on glass in 0.1 mM of $[Ru(NH_3)_6]Cl_3$ and 0.1 mM of ferrocenemethanol in 0.1 M Na_2SO_4. Initially the UME was positioned far from the surface, and then approached the surface with the help of the SECM setup by monitoring the steady-state current of Fc-MeOH oxidation at $E_T = 0.2$ V at the UME until the current stayed constant when the insulating sheath of the UME mechanically touched the surface. The UME was retracted 10 μm from this point for the pulse experiments. Subsequently the potential was switched to $E_T = -0.35$ V in order to reduce $[Ru(NH_3)_6]^{3+}$.

Acknowledgements

We are grateful for financial support from the Council for Chemical Sciences of the Netherlands Organization for Scientific Research (NWO-CW) (M. J. W. L; Vidi Vernieuwingsimpuls grant 700.52.423 to J. H.) and from the Lower Saxony-Israeli Foundation (Grant to G.W. No. ZN1744).

References

1 J. D. Swalen, D. L. Allara, J. D. Andrade, E. A. Chandross, S. Garoff, J. Israelchvili, T. J. McCarthy, R. Murray, R. F. Pease, J. F. Rabolt, K. J. Wynne and H. Yu, *Langmuir*, 1987, **3**, 932–950.
2 C. A. Bortolotti, G. Battistuzzi, M. Borsari, P. Facci, A. Ranieri and M. Sola, *J. Am. Chem. Soc.*, 2006, **128**, 5444–5451.
3 L. Andolfi, D. Bruce, S. Cannistraro, G. W. Canters, J. J. Davis, H. A. O. Hill, J. Crozier, M. Ph. Verbeet, C. L. Wrathmell and Y. Astier, *J. Electroanal. Chem.*, 2004, **565**, 21–28.
4 J. Zhao, J. J. Davis, M. S. P. Sansom and A. Hung, *J. Am. Chem. Soc.*, 2004, **126**, 5601–5609.
5 *Cytochrome c a multidisciplinary approach*, ed. R. A. Scott and A. G. Mauk, University Science books, Sausalito, California1996.
6 D. Keilin and E. F. Hartree, *Biochem. J.*, 1945, **39**, 289–292.
7 G. Battistuzzi, M. Borsari and M. Sola, *Antioxid. Redox Signaling*, 2001, **3**, 279–291.
8 G. Battistuzzi, M. Borsari and M. Sola, *Eur. J. Inorg. Chem.*, 2001, 2989–3004.
9 G. Battistuzzi, M. Borsari, F. Francia and M. Sola, *Biochemistry*, 1997, **36**, 16247–16258.
10 J. Deere, M. Serantomi, K. J. Edler, B. K. Hodnett, J. G. Wall and E. Magner, *Langmuir*, 2004, **20**, 532–536.
11 A. S. Haas, D. L. Pilloud, K. S. Reddy, G. T. Babcock, C. C. Moser, J. K. Blasie and P. L. Dutton, *J. Phys. Chem. B*, 2001, **105**, 11351–11362.
12 A. Fantuzzi, M. Fairhead and G. Gilardi, *J. Am. Chem. Soc.*, 2004, **126**, 5040–5041.
13 A. Fragoso, J. Caballero, E. Almirall, R. Villalonga and R. Caro, *Langmuir*, 2002, **18**, 5051–5054.
14 M. V. Rekharsky and Y. Inoue, *Chem. Rev.*, 1998, **98**, 1880–1901.
15 M. J. W. Ludden, D. N. Reinhoudt and J. Huskens, *Chem. Soc. Rev.*, 2006, **11**, 1122–1134.
16 S. Onclin, A. Mulder, J. Huskens, B. J. Ravoo and D. N. Reinhoudt, *Langmuir*, 2004, **20**, 5460–5466.
17 M. R. de Jong, J. Huskens and D. N. Reinhoudt, *Chem.–Eur. J.*, 2001, **7**, 4164–4170.
18 J. Huskens, M. A. Deij and D. N. Reinhoudt, *Angew. Chem., Int. Ed.*, 2002, **41**, 4467–4471.
19 T. Auletta, B. Dordi, A. Mulder, A. Sartori, S. Onclin, C. M. Bruinink, M. Péter, C. A. Nijhuis, H. Beijleveld, H. Schönherr, G. J. Vancso, A. Casnati, R. Ungaro, B. J. Ravoo, J. Huskens and D. N. Reinhoudt, *Angew. Chem., Int. Ed.*, 2004, **43**, 369–373.
20 M. J. W. Ludden, M. Péter, D. N. Reinhoudt and J. Huskens, *Small*, 2006, **2**, 1192–1202.
21 M. J. W. Ludden, A. Mulder, R. Tampé, D. N. Reinhoudt and J. Huskens, *Angew. Chem., Int. Ed.*, 2007, **46**, 4104–4107.
22 M. Brinkley, *Bioconjugate Chem.*, 1992, **3**, 2–13.
23 R. F. Latypov, H. Cheng, N. A. Roder, J. Zhang and H. Roder, *J. Mol. Biol.*, 2006, **357**, 1009–1025.
24 C. A. Nijhuis, J. K. Sinha, G. Wittstock, B. J. Ravoo and D. N. Reinhoudt, *Langmuir*, 2006, **22**, 9770–9775.
25 A. J. Bard, G. Denault and R. A. Friesner, *Anal. Chem.*, 1991, **63**, 1282–1288.
26 J. L. Amphlett and G. Denault, *J. Phys. Chem. B*, 1998, **102**, 9946–9951.
27 S. E. Pust, D. Scharnweber, S. Baunack and G. Wittstock, *J. Electrochem. Soc.*, 2007, **154**, C508–C514.
28 H. Schönherr, M. W. J. Beulen, J. Bügler, J. Huskens, F. C. J. M. van Veggel, D. N. Reinhoudt and G. J. Vancso, *J. Am. Chem. Soc.*, 2000, **122**, 4963–4967.
29 G. Bodo, *Biochim. Biophys. Acta*, 1957, **25**, 428–429.
30 N. L. Rosi and C. A. Mirkin, *Chem. Rev.*, 2005, **105**, 1547–1562.
31 Z. Ding, R. B. Fong, C. L. Long, P. S. Stayton and A. S. Hoffman, *Nature*, 2001, **411**, 59–62.
32 P. L. Edmiston and S. S. Saavedra, *J. Am. Chem. Soc.*, 1998, **120**, 1665–1671.
33 P. L. Edmiston, J. E. Lee, S.-S. Cheng and S. S. Saavedra, *J. Am. Chem. Soc.*, 1997, **119**, 560–570.
34 P. R. Ashton, R. Koniger, J. F. Stoddart, D. Alker and V. D. Harding, *J. Org. Chem.*, 1996, **61**, 903–908.
35 M. W. J. Beulen, J. Bügler, B. Lammerink, F. A. J. Geurts, E. M. E. F. Biemond, K. G. C. van Leerdam, F. C. J. M. van Veggel, J. F. J. Engbersen and D. N. Reinhoudt, *Langmuir*, 1998, **14**, 6424–6429.